

# 1 **Modelling the transmission dynamics of COVID-19 in six high** 2 **burden countries**

3

4 Azizur Rahman<sup>1\*</sup> and Md Abdul Kuddus<sup>2, 3</sup>

5

6 <sup>1</sup>*Data Science Research Unit, School of Computing and Mathematics, Charles Sturt University,*  
7 *Wagga Wagga, NSW, Australia*

8

9 <sup>2</sup>*Australian Institute of Tropical Health and Medicine, James Cook University, Townsville, QLD, Australia*

10

11 <sup>3</sup>*Department of Mathematics, University of Rajshahi, Rajshahi-6205, Bangladesh*

12

13 Corresponding author:

14 \*Azizur Rahman: [azrahman@csu.edu.au](mailto:azrahman@csu.edu.au)

15

16

17

18

19

20

21

22

23

24

25

26

27

28

29

30

31

32 **NOTE: This preprint reports new research that has not been certified by peer review and should not be used to guide clinical practice.**

33  
34  
35  
36  
37  
38  
39  
40  
41  
42  
43  
44  
45  
46  
47  
48  
49  
50  
51  
52  
53  
54  
55  
56  
57  
58  
59  
60  
61  
62  
63  
64  
65  
66  
67

## Abstract

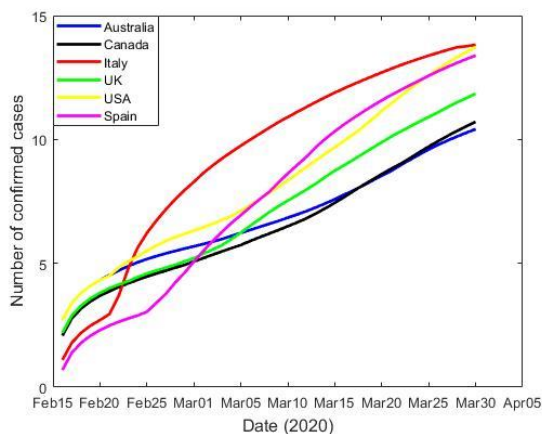
The new coronavirus disease, officially known as COVID-19, originated in China in 2019 and has since spread around the globe. We presented a modified *Susceptible-Latent-Infected-Removed* (SLIR) compartmental model of COVID-19 disease transmission with nonlinear incidence during the epidemic period. We provided the model calibration to estimate parameters with day wise corona virus (COVID-19) data i.e. reported cases by worldometer from the period of 15<sup>th</sup> February to 30<sup>th</sup> March, 2020 in six high burden countries including Australia, Italy, Spain, USA, UK and Canada. We estimate transmission rates for each countries and found that the highest transmission rate country in Spain, which may be increase the new cases and deaths in Spain than the other countries. Sensitivity analysis was used to identify the most important parameters through the partial rank correlation coefficient method. We found that the transmission rate of COVID-19 had the largest influence on the prevalence. We also provides the prediction of new cases in COVID-19 until May 18, 2020 using the developed model and recommends, control strategies of COVID-19. The information that we generated from this study would be useful to the decision makers of various organizations across the world including the Ministry of Health in Australia, Italy, Spain, USA, UK and Canada to control COVID-19.

**Keywords** Epidemic model, nonlinear incidence, transmission rate, COVID-19, simulations

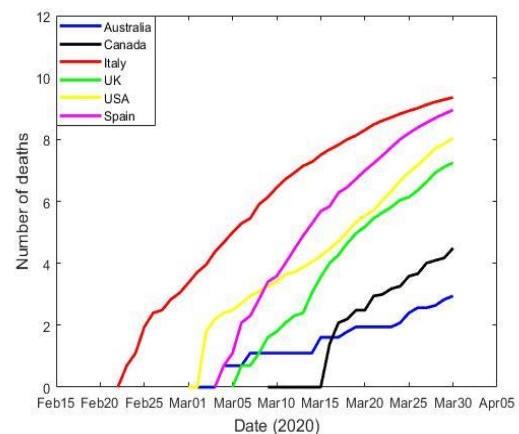
## 68 1. Introduction

69 Following the outbreak of novel Severe Acute Respiratory Syndrome Coronavirus-2 (SARS-  
70 Cov-2) or COVID-19 constitute a persistent and significant public-health problem across the  
71 globe. As of March 30th, 2020, the ongoing global epidemic outbreak of COVID1-19 has  
72 spread to at least 180 countries and territories on 6 countries including Australia, Italy, Spain,  
73 USA, UK and Canada, resulted approximately 946,876 cases of COVID-19, and 48,137  
74 individuals died from this disease [1]. In the Australia, Italy, Spain, USA, UK and Canada  
75 COVID-19 infection and death reached 4460, 101739, 87956, 163788, 22141 and 7448, as well  
76 as 30, 11591, 7716, 3143, 1408 and 89 with mortality ratios nearly 0.67%, 11.39%, 8.77%,  
77 1.9%, 6.4% and 1.2% respectively [1]. Figure 1 shows the cumulative number of confirmed  
78 cases and deaths of COVID-19 in six selected countries from February 15<sup>th</sup> to March 30<sup>th</sup>,  
79 2020.

(A)



(B)



80 Figure 1: Graphs of six selected countries using a log scale (A)–cumulative number of COVID-19 cases  
81 and (B)–cumulative number of COVID-19 deaths.

82

83 The highest burden of COVID-19 is not only dependent on the health system but also depend  
84 quickly response. For example, in Italy, the first confirmed COVID-19 cases on February 15  
85 and then after few days thousands of people infected by COVID-19. The problem is not that  
86 the Italy government didn't respond to the COVID-19. The problem is that it always responded  
87 slightly too slow and with slightly too much moderation. What has resulted in China reveals  
88 that quarantine, social distance, and isolation of infected populations can contain the epidemic.  
89 This impact of the COVID-19 response in China is advocating for many countries where  
90 COVID-19 is starting to spread. However, it is unclear whether other countries can implement  
91 the stringent measures China eventually adopted. Singapore and Hong Kong, both of which

92 had severe acute respiratory syndrome (SARS) epidemics in 2002–03, present concern and  
93 many lessons to other countries. In both places, COVID-19 has been maintained well to date,  
94 notwithstanding early cases, by early government progress and through social distancing  
95 patterns used by individuals.

96

97 The course of an epidemic is defined by a series of key factors, some of which are poorly  
98 understood at present for COVID-19. Mathematical modelling is one of the most powerful  
99 tools for infectious disease control that can be used for both predictions about behaviour and  
100 for understanding infectious disease dynamics [2-4]. Many researchers have implemented  
101 mathematical modelling frameworks to gain insights into different types of infectious diseases  
102 [5-9]. Although models can range from very simple to highly complex, one of the commonest  
103 practices to improve understanding of infectious disease dynamics is the compartmental  
104 mathematical model [10].

105

106 In mathematical models, the incidence rate plays an important role in the transmission of  
107 infectious diseases. The number of individuals who become infected per unit time is called the  
108 incidence rate in the epidemiology perspective [11]. Here, we consider the nonlinear incidence  
109 rate due to the number of effective contact between infective and susceptible individuals may  
110 saturate at high levels through the crowding of infectives individuals [12]. This model is also  
111 used to calibrate and make prediction the number of COVID-19 cases data in six countries  
112 including Australia, Italy, Spain, USA, UK and Canada to estimate the model parameters.  
113 Sensitivity analysis also performed to identify the most important model parameters that could  
114 potentially support policymakers to control COVID-19 outbreak in the selected countries. The  
115 model findings can be also helpful to many other countries which are dealing with critical  
116 outbreak of COVID-19.

117

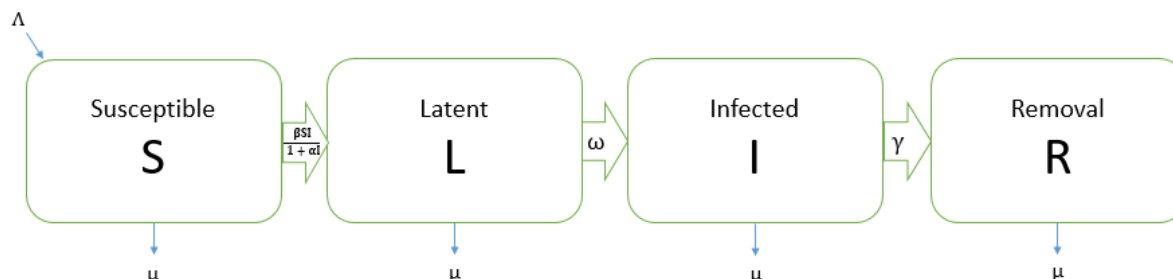
118 The rest of the paper is structured as follows: Section 2 presents model descriptions. Sections  
119 3 and 4 performed the model calibration and sensitivity analysis. A brief discussion and  
120 concluding remarks finalize the paper.

121

## 122 **2. Model description and analysis**

123 We considered a modified SLIR compartmental model of COVID-19 transmission with  
124 nonlinear incidence between the following mutually exclusive compartments:  $S(t)$ - susceptible

125 individuals; L(t)- latent individuals who have not yet progressed to active infection; I(t)-  
 126 infected individuals who are both infected and infectious, and R(t)-recovered individuals who  
 127 are previously infected but successfully recovered. A typical SLIR model is depicted in Figure  
 128 2.



129  
 130 Figure 2: Flow chart of the SLIR mathematical model showing the four states and the transitions in and  
 131 out of each state. Here, S = Susceptible population, L = Latent population, I = Infected population,  
 132 R = Removal population,  $\Lambda$  = recruited rate,  $\mu$  = Death rate,  $\beta$  = Transmission rate,  $\alpha$ =Force of  
 133 saturates infection,  $\omega$  = Progression rate to active disease,  $\gamma$  = Recovery rate.  
 134

135 Let the susceptible individuals be recruited at a constant rate  $\Lambda$  and they may be infected at a  
 136 time dependent rate  $\frac{\beta I(t)}{1+\alpha I(t)}$ . Here,  $\frac{\beta I(t)}{1+\alpha I(t)}$  is represents the saturated incidence rate, which  
 137 tends to a saturated level when I(t) gets large.  $\beta I(t)$  measures the force of infection when the  
 138 disease is entering a fully susceptible population, and  $\frac{1}{(1+\alpha I)}$  measures the inhibition effect from  
 139 the behaviour change of susceptible individuals when their number increase or from the effect  
 140 of risk factors including crowded environment of the infective individuals with  $\alpha$  determines  
 141 the level at which the force of infection saturates. Individuals in the different compartments  
 142 suffer from natural death at the same constant rate  $\mu$ . All infected individuals move to the  
 143 latently infected compartment, L(t). Those with latent infection progress to active infection  
 144 (the I compartment) as a result of reactivation of the latent infection at rate  $\omega$ . A proportion of  
 145 the infected individuals recover through treatment and natural recovery rate  $\gamma$  and move into  
 146 the recovered compartment R(t). In this case the model can be expressed by the following four  
 147 differential equations:

148  
 149 
$$\frac{dS}{dt} = \Lambda - \frac{\beta SI}{1+\alpha I} - \mu S, \tag{1}$$

150 
$$\frac{dL}{dt} = \frac{\beta SI}{1+\alpha I} - (\omega + \mu)L, \tag{2}$$

151 
$$\frac{dI}{dt} = \omega L - (\gamma + \mu)I, \tag{3}$$

152 
$$\frac{dR}{dt} = \gamma I - \mu R. \tag{4}$$

153

154 Given non-negative initial conditions for the system above, it is straightforward to show that  
155 each of the state variables remain non-negative for all  $t > 0$ . Moreover, summing equations  
156 (1)-(4) we find that the size of the total population,  $N(t)$  satisfies

$$157 \quad \frac{dN(t)}{dt} \leq \Lambda - \mu N.$$

158 Integrating this equation we find

$$159 \quad N(t) \leq \frac{\Lambda}{\mu} + N(0)e^{-\mu t}.$$

160 This shows that the total population size  $N(t)$  is bounded in this case, and naturally it follows  
161 that each of the compartment states (i.e.  $S$ ,  $L$ , and  $I$  etc.) are also bounded.

162

### 163 **3. Estimation of model parameters**

164 In this section we estimated the model parameters based on the available six countries COVID-  
165 19 reported cases data from the [worldometers.info](https://www.worldometers.info/) [1]. Figure 3 presents the curve of  
166 cumulative confirmed COVID-19 cases in each day during the period from the 15<sup>th</sup> February  
167 to 30<sup>th</sup> March 2020 in Australia, Italy, Spain, USA, UK and Canada. In order to parameterise  
168 the model (1) – (4), we obtained some of the parameter values from the literature (see, Table  
169 1), other were estimated or fitted from the data. The best-fitted parameter values were obtained  
170 by minimizing the error using least-square fitting method between the COVID-19 cases data  
171 and the solution of the proposed model (1) – (4) (see, blue solid graph in Figure 3).

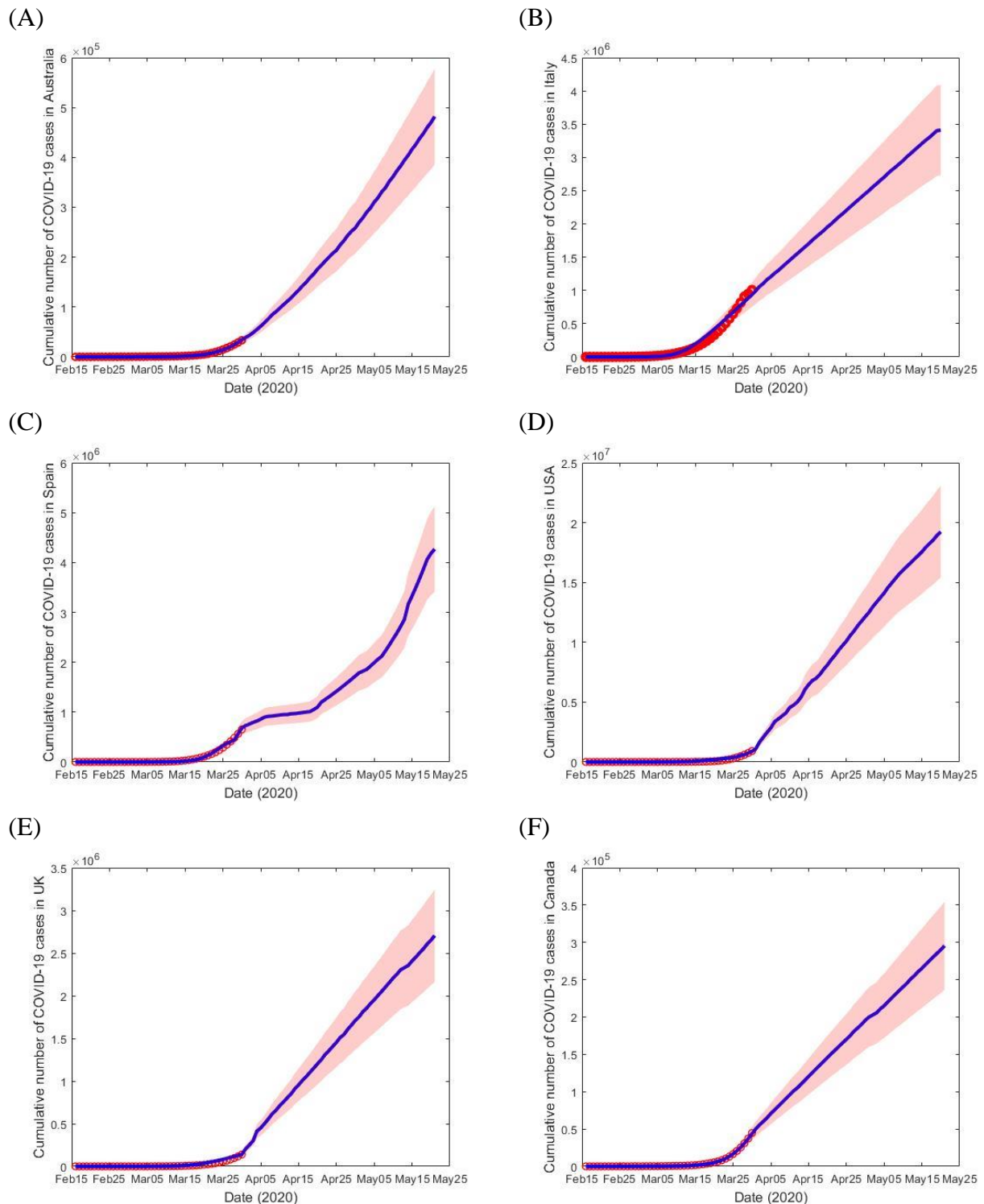
172

173 The objective function used in the parameter estimation is as follows

$$174 \quad \hat{\theta} = \operatorname{argmin} \sum_{i=1}^n (\omega L - \text{data}_{t_i})^2$$

175 where  $\text{data}_{t_i}$  denotes the COVID-19 data and  $\omega L$  are the corresponding model solution at  
176 time  $t_i$ , while  $n$  is the number of available actual data points. Findings reveal that the proposed  
177 model is well-fitted with the data.

178



179 Figure 3: Measured and predicted number of cumulative COVID-19 cases from February 15, 2020 to  
180 May 18, 2020 (red dot) in six different high burden countries (A) Australia, (B) Italy, (C) Spain, (D)  
181 USA, (E) UK and (F) Canada, and the corresponding model (blue solid curve) with the 95% confidence  
182 interval (CI) measure in the blue shaded limits.

183

184 The prediction results from the model are also depicted in Figure 3 to assist in evidenced based  
185 decision making process. For example, health department and decision makers including

186 political leaders of Australia, Italy, Spain, USA, UK and Canada those who bear the greatest  
 187 response for national health systems for what is predicted to happen in the days, weeks and  
 188 month to come. They can then implement measures regarding staff resources and hospital beds  
 189 to meet the challenges of this difficult time. However, if the number of infected individuals  
 190 follows this trend for the next month, there will be more than 400,000 in Australia, 350,000,0  
 191 in Italy, 400,000,0 in Spain, 180,000,00 in USA, 270,000,0 in UK and 300,000 in Canada  
 192 patients infected by May 18, as shown in Figure 3.

193

194 **Table 1:** Depiction and estimation of the model parameters for six countries

Countries	Parameters	Description	Estimated Values	References
<b>Australia</b>	N	Population in 2020	254,998,84	[13]
	$\mu$	Death rate	$\frac{1}{70} \text{ yr}^{-1}$	[14]
	$\beta$	Transmission rate	$1.3137 \times 10^{-7}$	Fitted
	$\omega$	Progression rate from L to I	0.01	Assumed
	$\gamma$	Recovery rate	0.1	Assumed
	$\alpha$	Infection saturates rate	0.00001	Assumed
	$\Lambda$	Recruitment rate	1	
<b>Italy</b>	N	Population in 2020	604,618,26	[15]
	$\mu$	Death rate	$\frac{1}{70} \text{ yr}^{-1}$	[14]
	$\beta$	Transmission rate	$2.5722 \times 10^{-8}$	Fitted
	$\omega$	Progression rate from L to I	0.00931	Assumed
	$\gamma$	Recovery rate	0.16	Assumed
	$\alpha$	Infection saturates rate	0.0000058	Assumed
	$\Lambda$	Recruitment rate	1	
<b>Spain</b>	N	Population in 2020	467,547,78	[16]
	$\mu$	Death rate	$\frac{1}{70} \text{ yr}^{-1}$	[14]
	$\beta$	Transmission rate	$6.7616 \times 10^{-7}$	Fitted
	$\omega$	Progression rate from L to I	0.00034	Assumed
	$\gamma$	Recovery rate	0.3	Assumed
	$\alpha$	Infection saturates rate	0.0000004	Assumed
	$\Lambda$	Recruitment rate	1	
<b>USA</b>	N	Population in 2020	331,002,651	[17]
	$\mu$	Death rate	$\frac{1}{70} \text{ yr}^{-1}$	[14]
	$\beta$	Transmission rate	$6.1269 \times 10^{-7}$	Fitted
	$\omega$	Progression rate from L to I	0.03	Assumed
	$\gamma$	Recovery rate	0.028	Assumed
	$\alpha$	Infection saturates rate	0.00000266	Assumed
	$\Lambda$	Recruitment rate	1	



<b>UK</b>	N	Population in 2020	678,869,11	[18]
	$\mu$	Death rate	$\frac{1}{70} \text{ yr}^{-1}$	[14]
	$\beta$	Transmission rate	$5.9950 \times 10^{-7}$	Fitted
	$\omega$	Progression rate from L to I	0.0003	Assumed
	$\gamma$	Recovery rate	0.1	Assumed
	$\alpha$	Infection saturates rate	0.00001	Assumed
	$\Lambda$	Recruitment rate	1	
<b>Canada</b>	N	Population in 2020	377,421,54	[19]
	$\mu$	Death rate	$\frac{1}{70} \text{ yr}^{-1}$	[14]
	$\beta$	Transmission rate	$4.5237 \times 10^{-7}$	Fitted
	$\omega$	Progression rate from L to I	0.0003	Assumed
	$\gamma$	Recovery rate	0.2	Assumed
	$\alpha$	Infection saturates rate	0.00001	Assumed
	$\Lambda$	Recruitment rate	1	

195

#### 196 **4. Sensitivity analysis**

197 Sensitivity analysis is performed to investigate the parameters that process the greatest  
 198 influence on the model outputs [20, 21]. In this study, we performed the partial rank correlation  
 199 coefficient (PRCC), which is a global sensitivity analysis technique proven to be the most  
 200 reliable and efficient sampling based method, is utilized [21, 22]. About 100,000 simulations  
 201 are performed and a uniform distribution is assigned to each model parameter and sampling is  
 202 performed independently. Positive (negative) correlations suggests that a positive (negative)  
 203 variation in the parameter will increase (decrease) the model outcome [21]. Here the model  
 204 outputs we consider are the number of infectious individuals  $I$  (where,  $I = \frac{\Lambda\beta\mu - \mu(\omega + \mu)(\gamma + \mu)}{(\omega + \mu)(\gamma + \mu)(\beta + \alpha\mu)}$ )  
 205 and the basic reproduction number  $R_0$  (where,  $R_0 = \frac{\Lambda\beta\omega}{\mu(\omega + \mu)(\gamma + \mu)}$ ). Figure 4 and Figure 5  
 206 display the correlation between  $I$  and  $R_0$  corresponding to the model parameters  $\beta$ ,  $\omega$ ,  $\alpha$  and  $\gamma$ .  
 207 Parameters  $\beta$  and  $\omega$  have positive PRCC values, implying that a positive change of these  
 208 parameters will increases the infectious individuals  $I$  and the basic reproduction number  $R_0$ . In  
 209 contract parameters  $\alpha$  and  $\gamma$  have negative PRCC values, which implies that increasing theses  
 210 parameters will decrease infectious individuals  $I$  and the basic reproduction number  $R_0$ .

211

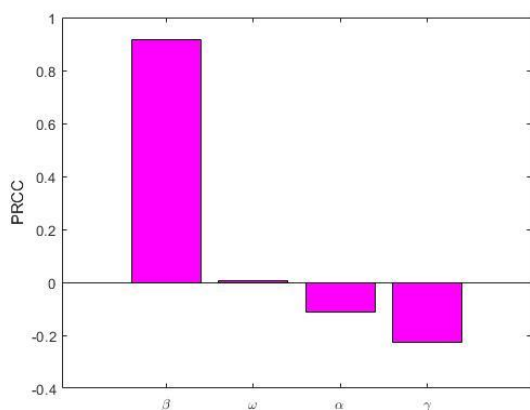


Figure 4: PRCC values depicting the sensitivities of the model output infectious individuals  $I$  with respect to the estimated parameters  $\beta$ ,  $\omega$ ,  $\alpha$  and  $\gamma$ .

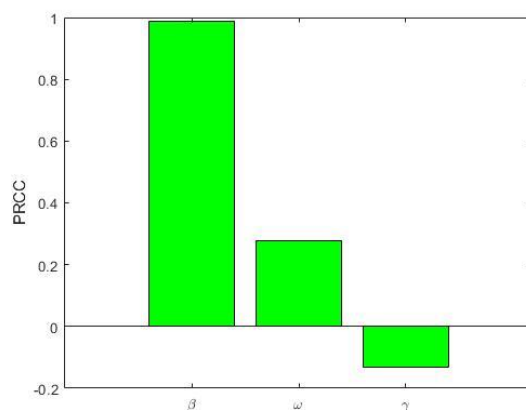


Figure 5: PRCC values depicting the sensitivities of the model output basic reproduction number  $R_0$  with respect to the estimated parameters  $\beta$ ,  $\omega$  and  $\gamma$ .

212

## 213 5. Discussion and Concluding remarks

214 In this paper, we presented a modified SLIR compartmental model with nonlinear incidence.  
215 We estimate number of cases from COVID-19 infection and apply it to data from the COVID-  
216 19 epidemics in Australia, Italy, Spain, USA, UK and Canada until 18 May 2020. After model  
217 calibration we estimates the transmission rates in Australia, Italy, Spain, USA, UK and Canada  
218 are  $1.3137 \times 10^{-7}$ ,  $2.5722 \times 10^{-8}$ ,  $6.7616 \times 10^{-7}$ ,  $6.1269 \times 10^{-7}$ ,  $5.9950 \times 10^{-7}$  and  
219  $4.5237 \times 10^{-7}$  respectively. The model estimates show a strong relationship with transmission  
220 rate and number of cases in COVID-19 of the selected countries.

221 Within the six different countries we found that Spain has the highest transmission rate than  
222 the other selected countries, which may be increase massive number of COVID-19 cases and  
223 make worst situation in Spain. We assume that initially Spain government may be not taken  
224 proper action to control transmission including handwashing, social distancing and good  
225 respiratory hygiene etc. For instance, in China they take immediate action for transmission  
226 control including lockdown in every cities that is way they are able to minimize the outbreak  
227 of COVID-19. Our finding is consistent with observations, because COVID-19 mainly spread  
228 from person to person through droplet transmission. Droplets are small pieces of saliva, which  
229 are produced when a person coughs or sneezes. Droplets cannot go through skin and can only  
230 lead to infection if they touch your mouth, nose or eye. Therefore, from a public health  
231 perspective it is very important to protect susceptible individuals from TB exposure by  
232 effectively reducing the contact rate between susceptible and infectious individuals.

233 There are so many ways that we can control COVID-19 transmission (i) wash your hands  
234 regularly with soap and water or rubbing an alcohol-based sanitizer into your hands because  
235 washing your hands kills viruses that may be on your hands, (ii) avoid touching your face as  
236 much as possible because virus containing droplets on your hands can be transferred to your  
237 eyes, mouth or nose where they can infect you, (iii) maintain at least 1.5 meters distance  
238 between yourself and anyone who is coughing or sneezing because if you are too close to  
239 someone you might breathe in droplets they cough or sneeze, (iv) make sure you and people  
240 around you follow good respiratory hygiene. Respiratory hygiene is important because droplets  
241 spread virus. By following good respiratory hygiene you catch any droplets that might be  
242 produced, and this protects the people around you from viruses including COVID-19. (v) Must  
243 wear a mask if you are sick with symptoms that might be due to COVID-19 or looking after  
244 someone who may have COVID-19.

245 However, estimation of transmission rates from different setting must be done with caution, as  
246 the pattern of an epidemic, the standard of care and, as a result, number of cases are time and  
247 setting dependent. For instance, very few cases have been reported so far in Bangladesh [23].  
248 In this country, health system is very poor which leads to the fewer number of reported cases.  
249 Therefore, data from other countries, in particular the number of cases by date of COVID-19  
250 onset is necessary to better understand the variability in cases across settings.

251 Our model determined that from the explicit expression for infectious individuals  $I$  and the  
252 basic reproduction number  $R_0$ , it is clear that they are depending on transmission rates  $\beta$ ,  
253 progression rates  $\omega$ , recovery rates  $\gamma$ , and the force of infection saturates rate  $\alpha$ . From the  
254 sensitivity analysis it is also clear that the most important parameter is transmission rate  $\beta$   
255 followed by recovery rate  $\gamma$ . Therefore, to control and eradicate COVID-19 infection, it is  
256 important to consider the following strategies: (i) the first and most important strategy is to  
257 minimize the contact rates  $\beta$  with infected individuals by decreasing the values of  $\beta$ ; (ii) the  
258 second-most important strategy is to increase the recovery rate  $\gamma$  of infective individuals  
259 through treatment. Therefore, we suggest the most feasible and optimal strategy to eliminate  
260 COVID-19 in six different countries including Australia, Italy, Spain, USA, UK and Canada  
261 are to reduce contact rates as well as increase the treatment rate that will be most effective way  
262 to reduce COVID-19 cases in the six countries. Finally, the application of proposed model and  
263 its related outputs can be extended into many other countries which are dealing with such a  
264 critical outbreak of COVID-19 to control this global pandemic disease.

265

## 266 **Ethical approval**

267 This study based on aggregated COVID-19 surveillance data in Australia, Italy, Spain, USA,  
268 UK and Canada taken from the worldometer. No confidential information included because  
269 analyses were performed at the aggregate level. Therefore, no ethical approval is required.

270

## 271 **Data availability statement**

272 All data will be available upon request.

273

## 274 **Contributors**

275 AR conceived, designed and supervised the study. MAK contributed to the literature search  
276 and data collection. AR and MAK contributed to data analysis, table and figures,  
277 interpretation of results and writing of the manuscript.

278

## 279 **Funding**

280 This work was not funded and did not receive any specific grant from funding agencies in the  
281 public, commercial, or not-for profit sectors.

282

## 283 **Acknowledgments**

284 The authors would like to thank the editorial office for their quick response and valuable  
285 comments to produce the updated version.

286

## 287 **Conflict of Interest**

288 The authors declare that there are not conflicts of interest.

289

## 290 **References**

- 291 [1] Worldometer, Coronavirus cases and deaths, Dover, Delaware, U.S.A. (2020).  
292 [2] R.J. Maude, Y. Lubell, D. Socheat, S. Yeung, S. Saralamba, W. Pongtavornpinyo, B.S. Cooper, A.M.  
293 Dondorp, N.J. White, L.J. White, The role of mathematical modelling in guiding the science and  
294 economics of malaria elimination, *International Health* 2(4-6) (2010) 239-246.  
295 [3] A.J. Kucharski, T.W. Russell, C. Diamond, Y. Liu, J. Edmunds, S. Funk, R.M. Eggo, C.n.w. group,  
296 Early dynamics of transmission and control of COVID-19: a mathematical modelling study, *medRxiv*  
297 (2020).  
298 [4] A. Remuzzi, G. Remuzzi, COVID-19 and Italy: what next?, *The Lancet*.  
299 [5] L.J. White, Flegg, J. A., Phyo, A. P., Wiladpai-ngern, J. H., Bethell, D., Plowe, C., Anderson, T.,  
300 Nkhoma, S., Nair, S., Tripura, R., Stepniewska, K., Pan-Ngum, W., Silamut, K., Cooper, B. S., Lubell, Y.,

- 301 Ashley, E. A., Nguon, C., Nosten, F., White, N. J., Dondorp, A. M., Defining the in vivo phenotype of  
302 artemisinin-resistant falciparum malaria: a modelling approach, *PLoS medicine* 12(4) (2015)  
303 e1001823.
- 304 [6] R.J. Maude, Pontavornpinyo, W., Saralamba, S., Aguas, R., Yeung, S., Dondorp, A. M., Day, N. P.,  
305 White, N. J., White, L. J., The last man standing is the most resistant: eliminating artemisinin-  
306 resistant malaria in Cambodia, *Malaria Journal* 8 (2009) 31.
- 307 [7] J.M. Trauer, Ragonnet, R., Doan, T. N., McBryde, E. S., Modular programming for tuberculosis  
308 control, the "AuTuMN" platform, *BMC Infectious Diseases* 17(1) (2017) 546.
- 309 [8] R. Ragonnet, Trauer, J. M., Denholm, J. T., Marais, B. J., McBryde, E. S., A user-friendly  
310 mathematical modelling web interface to assist local decision making in the fight against drug-  
311 resistant tuberculosis, *BMC Infectious Diseases* 17(1) (2017) 374.
- 312 [9] E.S. McBryde, Meehan, M. T., Doan, T. N., Ragonnet, R., Marais, B. J., Guernier, V. Trauer, J. M.,  
313 The risk of global epidemic replacement with drug-resistant *Mycobacterium tuberculosis* strains,  
314 *International Journal of Infectious Diseases* 56 (2017) 14-20.
- 315 [10] C.I. Siettos, Russo, L., Mathematical modeling of infectious disease dynamics, *Virulence* 4(4)  
316 (2013) 295-306.
- 317 [11] J.P. Vandenbroucke, N. Pearce, Incidence rates in dynamic populations, *International journal of*  
318 *epidemiology* 41(5) (2012) 1472-1479.
- 319 [12] X.-Z. Li, W.-S. Li, M. Ghosh, Stability and bifurcation of an SIR epidemic model with nonlinear  
320 incidence and treatment, *Applied Mathematics and Computation* 210(1) (2009) 141-150.
- 321 [13] Worldometer, Population of Australia, Dover, Delaware, U.S.A. (2020).
- 322 [14] Y. Yali, et al., Global stability of two models with incomplete treatment for tuberculosis, *Chaos,*  
323 *solutions & fractals* 43 (2010) 79-85.
- 324 [15] Worldometer, Population of Italy, Dover, Delaware, U.S.A. (2020).
- 325 [16] Worldometer, Population of Spain, Dover, Delaware, U.S.A. (2020).
- 326 [17] Worldometer, Population of the United States, Dover, Delaware, U.S.A. (2020).
- 327 [18] Worldometer, Population of United Kingdom, 2020, Dover, Delaware, U.S.A. (2020).
- 328 [19] Worldometer, Population of Canada, 2020, Dover, Delaware, U.S.A. (2020).
- 329 [20] A. Rahman, A. Kuddus, Cost-effective modeling of the transmission dynamics of malaria: A case  
330 study in Bangladesh, *Communications in Statistics: Case Studies, Data Analysis and Applications*  
331 (2020) 1-17.
- 332 [21] S. Kim, A. Aurelio, E. Jung, Mathematical model and intervention strategies for mitigating  
333 tuberculosis in the Philippines, *Journal of theoretical biology* 443 (2018) 100-112.
- 334 [22] J.B. Njagarah, F. Nyabadza, Modelling optimal control of cholera in communities linked by  
335 migration, *Computational and mathematical methods in medicine* 2015 (2015).
- 336 [23] Worldometer, Total Coronavirus Cases in Bangladesh, Dover, Delaware, U.S.A. (2020).

337